Comparison of three Kirchhoff integral formulas for true amplitude inversion

Hassan Khaniani, Gary F. Margrave and John C. Bancroft

ABSTRACT

Estimation of reflectivity is an objective of true amplitude inversions. True estimation of reflectivity requires removing other influences on amplitude of the wavefield than reflectivity (e.g., geometrical spreading). This work summarizes and compares the literatures for three different theoretical approaches for true amplitude Kirchhoff depth migration inversion. These approaches are using paraxial ray theory, inverse scattering and applying imaging condition on downward continuation of seismic data. To provide a comparison, in the final section weight functions are compared for a common source configuration, using a constant velocity model. The result shows that they are very similar.

INTRODUCTION

Seismic data can be thought of as containing two main types of information: traveltime and amplitude. The traveltime for a particular reflection event in a single seismogram is the total time taken by the impulse of source energy as it propagates from the source location to the reflector element and back to the receiver location. According to Fermat's principle traveltime information can be obtained from the travel path of the ray and its wavespeed. The amplitude of the reflection event provides information about the strength of the reflectivity of the reflectors. Several factors influence the amplitude of seismic records such as attenuation, reflection, transmission and geometrical spreading factor. (Cerveny, 1993). According to Sun (Sun et al., 1998) the term true-amplitude migration is a new development of Kirchhoff-type migration that uses proper weighting function in the diffraction stack integral to construct the source pulse proportional to reflectivity. This paper serves as an introduction to the mathematics of seismic migration and inversion problem. The forward model operator can be the Kirchhoff Helmholtz Integral (KHI) that generates observed wavefield by superposition of Huygens elementary waves located along the reflector surface and explodes in response to the incident wave with secondary-source strengths proportional to the local reflectivity. The inverse problem estimates the reflectivity of the reflectors. In recent years attempts have been made to solve the inverse problem in different strategies. Three of them will be considered.

The first strategy is based on zero-order paraxial ray theory that developed by Schelicher (1993) . He considered one central ray that belongs to a primary reflected elementary elastic wave that crosses a certain number of interfaces on its path to reflector point and after being reflected, traverses another number of interfaces on its path to the receiver. Then he used zero order ray theory to describe paraxial rays in vicinity of central ray with the same wave mode that pass through same layer and interfaces. He achieved a complex weight function that accounts for caustics along the ray path.

The second strategy comes from scattering theory that is a framework for studying and understanding of the scattering of waves and particles. Beginning with Beylkin (1985) and continued by Bleistein et al. (1985, 1987, 1987a, 1987b) it uses perturbation theory that comprises mathematical methods that are used to find an approximate solution to a problem which cannot be solved exactly, by starting from the exact solution (i.e., Green functions). The solved, but simplified problem is then "perturbed" to make the conditions such that the perturbed solution actually converges closer to the real problem. In this way background wavespeed profile v(x) is represented as small perturbation from background profile c(x). Then the nonlinear equation is linearized by use of the Born approximation that consists of taking the incident wavefield in medium of the total wavefield as the driving field at each scatterpoint. It is accurate if the scattered field is small, compared to the incident field, in the scatter points.

The third strategy is published by Docherty (1991) that is to backward propagate the reflected wavefield by replacing the retarded Green's function with an advanced one. In other words, advanced Huygens waves recorded in measurement surface is reversed (propagated downward) to its (possible) scatter points. If this wave is considered with elementary-wave propagated from a common-source and a suitable imaging condition, the reflector can be imaged.

All three approaches give similar weighting function that could be proved analytically, however, as an example they are compared for a simple model of flat laterally homogeneous medium and similar weighting function obtained.

FORWARD MODELING

To describe any paraxial ray, as well as the amplitude and traveltime associated with paraxial ray family three local coordinate systems are used. The first one is defined as the source ccordinate system with its origin at a certain source point. This coordinate system is used to describe the source positions. The second coordinate system is called receiver coordinate system with its origin at certain receiver point. This coordinate system is needed to locate every receiver point. The third coordinate system is attached to the target reflector with its origin at reflection point under consideration. The term reflection coordinate system is used because every reflection point is given in this coordinate. The dislocation vector between source position located at x_s to the next source position $\overline{x_s}$, the receiver position x_g to the next receiver point $\bar{x}_g$ and the reflection point x to the next reflection point $\bar{x}$ are denoted by $s = (x_{S1}, x_{S2})$, $g = (x_{g1}, x_{g2})$ and $x_r = (x_1, x_2)$ respectively. The surface is parameterized by two variables ξ_1, ξ_2(i.e., $\xi \equiv (\xi_1 , \xi_2)$) (Schleicher ,1993 , Sun et al.,1997).

The propagation of scalar wavefield $\psi(x, x_s, \omega)$ at an observation point x by a source position x_s can be described using scalar wave equation(SWE) that can be expressed in form of Helmholtz equation

$$\left[\nabla^2 + \frac{\omega^2}{v^2(x)}\right] \hat{\psi}(x, x_s, \omega) = -F(\omega)\delta(x - x_s), \tag{1}$$

where $v(x)$ is wavespeed of the medium and source impulse is denoted by $\delta(x - x_s)$ which is located in position x_s. The term $F(\omega)$ denotes frequency spectrum of source.

The total field $\hat{\psi}(x, x_s, \omega)$ can be expressed as the sum of an incident field and scattered field,

$$\hat{\psi}(x, x_s, \omega) + \hat{\psi}_I(x, x_s, \omega) + \hat{\psi}_s(x, x_s, \omega). \tag{2}$$

The classical Kirchhoff integral (Sommerfield,1964) represents a time harmonic acoustic scattered wavefield $\psi_s(x_g, x_s, \omega)$ at receiver point x_g in terms of that wavefield and an Green's function of incident wavefield $\psi_I(r, x_s, \omega)$ originated from x_s, and its normal derivative, known at all points x on a given smooth surface $\sum$ that encloses receiver locations. The primary sources are assumed to lie inside $\sum x_g$ while the secondary sources $\sum x$ (scatterers) are assumed to be outside of $\sum x_g$(see Figure 1).

With this understanding the standard acoustic Kirchhoff integral may be written by implementation of Green's theorem (Shearer, 1999, Schleicher et al., 2007):

$$\psi_s(x_g, x_s, \omega) \sim \frac{-1}{4\pi} \int_{\sum x} \rho {v_M^+}^2 [g(x, x_g, \omega) \frac{\partial \psi_s(x, x_s, \omega)}{\partial n} - \psi_s(x, x_s, \omega) \frac{\partial g(x, x_g, \omega)}{\partial n}] dx^2. \tag{3}$$

where ρ and υ are density and velocity and the operator $\partial/\partial n = n.\nabla$ denotes the normal derivative in the direction of *n*. Immediately after reflection, the approximated reflected wave is field is obtained by

$$\psi_s(x, x_s, \omega) = \bar{R}_C \psi_I(x, x_s, \omega), \tag{4}$$

where the factor $\bar{R}_C$ is the reciprocal reflection coefficient at the target reflector which is defined by

$$\bar{R}_C = \left(\frac{\varrho^+ \upsilon^+ \cos \vartheta_k^+}{\varrho^- \upsilon^- \cos \vartheta_k^-} \right)^{\frac{1}{2}} R_C, \tag{5}$$

where, ϑ is ray propagation angle as depicted in Figure 2. The superscripts + and – shows the situation of the incident and outgoing ray properties respectively. For our study as KHI deals with scalar wave equation and assuming monotypic wave (P-P or S-S) so we have $\bar{R}_C = R_C$. By estimating the normal derivatives of functions g and ψ_s and by zero order ray approximation in equation (3) KHI can be obtained:

$$\psi_s(r, x_s, \omega) \sim \frac{i\omega}{2\pi} \int_S \ dx^2\, K_{kH} \bar{R}_C e^{-i\omega \phi_D(x,\xi)}, \tag{6}$$

where, $\phi_D(x, \xi)$ is diffraction traveltime obtained by sum of traveltimes from source to a scatterpoint $\tau_s(x, x_s)$ and from scatterpoint to the receiver location $\tau_g(x, x_g)$ as

$$\phi_D(x, \xi) = \tau_s(x, x_g(\xi)) + \tau_g(x, x_s(\xi)). \tag{7}$$

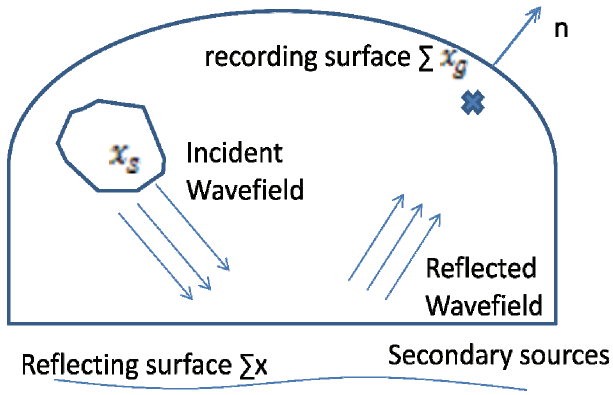

FIG. 1.Geometry of incident and reflected wavefield for application of Green's theorem (modified from Schleicher et al., 2007)

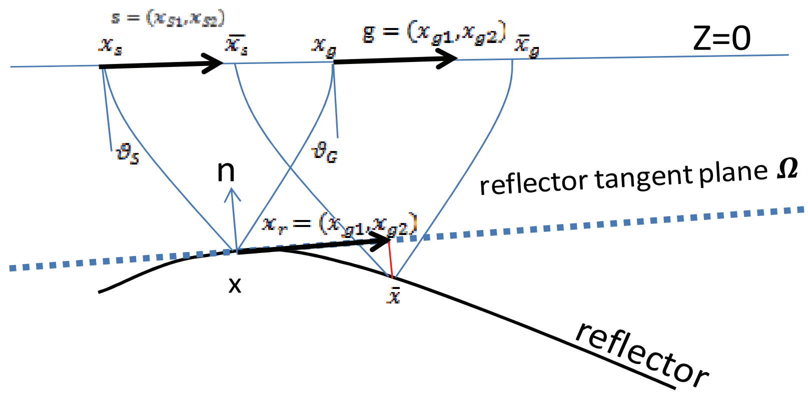

FIG. 2. Three coordinate systems for description of dislocation of sources s, receivers g and reflection point x_r. n is the normal vector on a the plane $\boldsymbol{\Omega}$. Here indicated for constant offset configuration.(modified from Schleicher et al., 1993)

In deriving equation (6) from (3) the following relationships were used :

$$g(x, x_g, \omega) \sim A(x, x_g) e^{-i\omega\tau_g(x, x_g)}, \tag{8}$$

$$\psi_I(x, x_s, \omega) \sim F(\omega) A(x, x_s) e^{-i\omega\tau_s(x, x_s)}, \tag{9}$$

$$\frac{\partial \psi_s(x, x_s, \omega)}{\partial n} = i\omega \frac{\cos \vartheta_M^+}{v_M^+} \psi_s(x, x_s, \omega), \tag{10}$$

$$\frac{\partial g(x, x_g, \omega)}{\partial n} = \left(-i\omega \frac{\cos \vartheta_M^G}{v_M^+}\right) g(x, x_s, \omega) \tag{11}$$

and forward weight function K_{kH} is defined as

$$K_{kH} = \rho {v_M^+}^2 A(x, x_g) A(x, x_s) \frac{\cos \vartheta_M^+ + \cos \vartheta_M^G}{2 v_M^+}, \tag{12}$$

where the term $A(x, x_s)$ is asymptotic in-plane Green's function amplitude and is derived using Eikonal and transport equations as

$$A(x, x_s) = \frac{1}{4\pi|q'\sigma K|^{\frac{1}{2}}} \ , \tag{13}$$

where q' denotes initial value of vertical component of slowness, σ is a ray parameter which is related to arc length along rays, and K is in-plane ray Jacobian (Bleistein et al., 1987). If the background velocity is assumed to be constant the solution of equation (13) can be

$$A(x, x_s) = \frac{1}{|x - x_s|'} \ , \tag{14}$$

and similarly for variables with subscript g replacing subscript s to describe receivers Green function (Bleistein et al., 1987).

Equation (3) obtained by assuming that both source and receivers lie on a given measurement configuration surface ξ. As a description the KHI is considered as a forward problem that generates observed wavefield $\psi_s(x_g, x_s, \omega)$ by superposition of Huygens elementary (diffracted) waves located along the reflector and exploded in response to the incident wave with secondary-source strengths proportional to the local reflection coefficient. Time domain expression of the equation (3) is skipped here but in practice, this formula is a basis for many computer programs that compute Kirchhoff synthetic seismograms.

In equation (6), $\phi_D(x, \xi)$ is a function of surface coordinates (i.e., $\phi_D(\xi)$). Changing ξ produces a change in $\phi_D(x, \xi)$, meaning that in high frequency ω, the exponential term $e^{-i\omega(\phi_D(x,\xi))}$ oscillates rapidly as ξ changes. This will cause a cancelling effect by cancelling positive areas by negative areas inside integral equation that will give little or no contribution to the integral. However, at a stationary point x_R that $\phi(\xi)$ does not change if ξ changes then $e^{-i\omega(\phi_D(x,\xi))}$ does not oscillates with ξ. Hene there is no cancelling effect, giving significant contribution to the integral. The main contribution to the integral comes from such a zone surrounding x_R that the phase $\phi_D(\xi)$ is stationary (Krebes, 2009).

By a high-frequency approximation the asymptotic evaluation of KHI at stationary point x_R the diffraction and reflection traveltime coincides (ie. $\phi_D(x, x_R) = \phi_R(\xi)$) and we replace $\phi_D(x, x_R)$ with $\phi_R(\xi)$ to get (Cerveny, 1985, Bleistein, 1984, Cerveny, 2001):

$$\psi_s(\xi, t) = \bar{R}_C \frac{\mathcal{A}}{\mathcal{L}} F[t - \phi_R(x, \xi)]. \tag{15}$$

Note that the analytic point-source wavelet *F[t]* is defined by

$$F[t] = f(t) + i\mathcal{H}\{f[t]\}, \tag{16}$$

where $\mathcal{H}$ is Hilbert transform operator. The source wavelet *f[t]* is assumed to be causal pulse and is assumed to be the same for all source and receiver pairs and vanishes outside an interval $0 \le t \le \gamma_\varepsilon$ where γ_ε is the length of that wavelet.

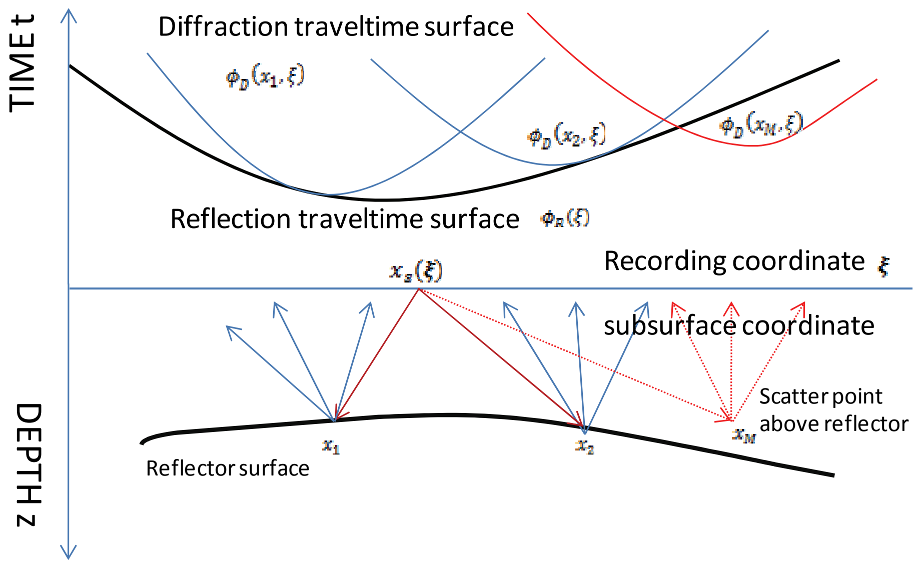

FIG. 3. 2-D sketch of the two traveltime surfaces $\phi_R(\xi)$ and $\phi_D(x,\xi)$. Here indicated for common shot configuration.

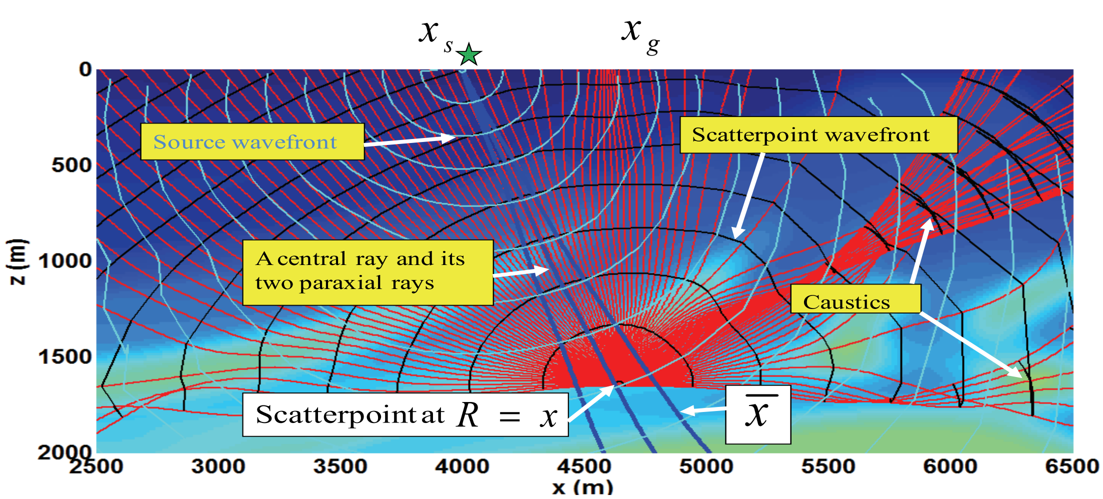

FIG. 4. Simulation for the ray paths and wavefronts of the a wave that initiates from a source, then diffracts to the receivers. The velocity is taken from Marmousi model. Note the behaviour of wavefronts and the caustics that it experiences.

The parameter $\mathcal{A}$ is to express the total transmission loss along the ray $x_s x x_g$ that are due to all discontinuity in 3D medium that are caused by velocity and density changes and is defined by

$$\mathcal{A} = \frac{S_s}{\sqrt{\varrho_g v_g^2 \varrho_s v_s^2}} \prod_{\substack{k=1 \\ k \neq j}}^{n} \left(\frac{\varrho^+ v^+ \cos \vartheta_k^+}{\varrho^- v^- \cos \vartheta_k^-} \right)^{\frac{1}{2}} T_K, \tag{17}$$

where S_s is source strength and subscripts g and s is to specify location of source and receiver density and velocity. $\bar{T}_K$ is the reciprocal transmission coefficient at k^{th} interface (Cerveny, 2001)

$$\bar{T}_K = \left(\frac{\varrho^+ v^+ \cos\vartheta_k^+}{\varrho^- v^- \cos\vartheta_k^-}\right)^{\frac{1}{2}} T_K, \tag{18}$$

Finally the important term $\mathcal{L}$ is normalized geometric- spreading factor that is defined by

$$\mathcal{L} = \sqrt{\frac{\cos\vartheta_S \cos\vartheta_G}{v_S v_G}} \frac{1}{\sqrt{\left|\det \widetilde{H}_{\mathrm{F}}\right|}} e^{-i(\frac{\pi}{2})k}, \tag{19}$$

where k is number of caustic encountered along the ray from starting point to its end point. The value of $\mathcal{L}$ is unaltered when the position of source and receiver are interchanged. $\widetilde{H}_{\mathrm{F}}$ is Hessian 2×2 matrix which is a second derivative operator of ϕ_F with respect to ξ_1 and ξ_2

$$\widetilde{H}_{\mathrm{F}} = \left|\left(\frac{\partial^2\phi_R(\xi)}{\partial\xi_i\partial\xi_j}\right) - \left(\frac{\partial^2\phi_D(\xi, M)}{\partial\xi_i\partial\xi_j}\right)\right|, \tag{20}$$

and $\phi_F(\xi; M)$ is defined as

$$\phi_F(\xi; M) = \phi_D(\xi; M) - \phi_R(\xi). \tag{21}$$

Therefore superposition of all energy that originated along reflector have constructive interface at stationary point and the constructive interface and align itself with the seismic reflection traveltime surface $\phi_R(\xi)$. Figure 3 shows the sketch of $\phi_R(\xi)$ and diffraction traveltime surface $\phi_D(x, \xi)$. Both traveltimes depends on the source and receiver pair and the tangent point happens when x_M lay on reflection surface.

The ray paths from a common source configuration are simulated in Figure 4. The velocity is taken from Marmousi model to show the behaviour of wavefronts and the caustics that they experience along their path. The blue color rays from source can be thought of as a central ray and paraxial rays that have the same wave mode that pass through same layer and interfaces.

KIRCHHOFF INVERSION BY PARAXIAL RAY THEORY

A true-amplitude migration can be performed using a certain Diffraction-Stack Integral (DSI) and deriving a weighted function from it. Schleicher et al. (1993) derived the following time domain DSI equation to obtain diffraction-stack migration output

$$\mathrm{v(x,t)} = \frac{-1}{2\pi} \iint\limits_A d^2\xi\, K_{DS}(\xi; x) \frac{\partial\psi_s\big(\xi, t + \phi_D(x, \xi)\big)}{\partial t}. \tag{22}$$

In the above equation $K_{DS}(\xi;x)$ is weight function that is yet to be found. Note that the derivative of equation(15) is used in equation (22):

$$\frac{\partial\psi_s\big(\xi,t+\phi_D(x,\xi)\big)}{\partial t}=\frac{\partial\bar{R}_C\frac{\mathcal{A}}{\mathcal{L}}F[t+\phi_D(x,\xi)-\phi_R(\xi)]}{\partial t}. \tag{23}$$

In actual migration, the stacks are performed only when t=0 (Schleicher, 2007). The result of integral equation are considerably different values when point x is an actual reflection point versus it is not (see Figure 3). If the appropriate values of weighted functions are determined, the stack in above integral removes the geometric-spreading factor $\mathcal{L}$ from primary reflections. Using equation (21) and transforming (22) to the frequency domain we get

$$\hat{\mathrm{v}}(\mathrm{x},\omega)=\hat{\mathrm{F}}[\omega]\frac{-i\omega}{2\pi}\iint_A d\xi_1 d\xi_2\,K_{DS}(\xi;x)\frac{\bar{R}_C}{\mathcal{L}}\exp[i\omega\phi_F(\xi;x)], \tag{24}$$

where $\hat{\mathrm{F}}[\omega]$ and $\hat{\mathrm{v}}(\mathrm{x},\omega)$ denotes the fourier transform of $F[t]$ and $\mathrm{v}(\mathrm{x},\mathrm{t})$ respectively.

In inhomogeneous media the above equation cannot be solved by using analytical method, but it can be approximated for high frequencies by using the stationary-phase method. In equation (24) by setting $\nabla_\xi\phi_F(\xi;x)=o$ it is possible to approximate $\phi_F(\xi;x)$ by use of Taylor series expansion up to the second order with a stationary point x_R (see eg. Cerveny,2001)

$$\phi_F(\xi;x)=\phi_F(x_R;x)+\frac{1}{2}(\xi-x_R).\widetilde{H}_{\mathrm{F}}.(\xi-x_R). \tag{25}$$

Equation(24) under assumption of high frequency and 2D stationary phase method can be

$$\hat{\mathrm{v}}(\mathrm{x},\omega)\approx\check{\mathrm{F}}[\omega]\,K_{DS}(x_R;x)\frac{\bar{R}_C}{\mathcal{L}\sqrt{|\det\widetilde{H}_{\mathrm{F}}|}}\times\exp\left\{i\omega\phi_F(\xi;x)-\frac{i\pi}{2}\left[1-\frac{Sgn(\widetilde{H}_{\mathrm{F}})}{2}\right]\right\}. \tag{26}$$

In above equation $Sgn(\widetilde{H}_{\mathrm{F}})$ is the signature of $\widetilde{H}_{\mathrm{F}}$ as defined by

$$Sgn\big(\widetilde{H}_{\mathrm{F}}\big)=sgn(\lambda_1)+sgn(\lambda_2), \tag{27}$$

where λ_1 and λ_2 are the real nonzero eigenvalues of the $\widetilde{H}_{\mathrm{F}}$. Also note that $\mathrm{sgn}(\big(\lambda_j\big)=\pm1$ according to whether $\lambda_j>0$ or $\lambda_j<0$ (see e.g., schleicher, 1993 and 2007, Creveny, 2001).

Schleicher (1993) derived a weight function $K_{DS}(x_R;R)$ for a reflection point R that has x_sRx_g ray path then he generalized his weight function to all points in reflector coordinates points x using paraxial ray theory. His final weight formula is

$$K_{DS}(\xi;\mathrm{x})=\sqrt{\frac{\cos\vartheta_S\cos\vartheta_G}{v_Sv_G}}\frac{\left|\det\,(\Gamma_S^{\mathrm{T}}\mathrm{N}_{\mathrm{Sx}}+\Gamma_G^{\mathrm{T}}\mathrm{N}_{\mathrm{Gx}}\right|}{\sqrt{|\det\,(N_{Sx}|}\sqrt{|\det\,(N_{Gx}|}}\exp\left\{-\frac{i\pi}{2}(\kappa_S+\kappa_G)\right\}, \tag{28}$$

where the following relationship for x_sRx_g were implemented:

$$\sqrt{\left|\det \widetilde{H}_{\mathrm{F}}\right|} = \frac{\left|\det (\Gamma_{S}^{T}N_{SR} + \Gamma_{G}^{T}N_{GR}\right|}{\sqrt{\left|\det (N_{R}^{S} + N_{R}^{G})\right|}}, \tag{29}$$

and the term κ is defined as:

$$\kappa = \kappa_S + \kappa_G + [1 - Sgn(\frac{\breve{H}_F}{2})], \tag{30}$$

where κ_S and κ_G are number of caustics along the two-way branches. Γ_S and Γ_G denote 2×2 measurment configuration matrices that depends and represents the source receive acquisition geometry as a function of ξ (Schleicher et al., 2001) .Then the second derivative of matrixes of traveltime function N_G^S and N_S^G, are computed by

$$N_G^S = \left(\frac{\partial^2 \phi_D(x_g, x_s)}{\partial x_{gi} \partial x_{gj}}\right), \mathrm{g} = 0 \text{ for } \mathrm{i} = 1,2, \tag{31}$$

and

$$N_S^G = \left(\frac{\partial^2 \phi(x_s, x_g)}{\partial x_{si} \partial x_{sj}}\right), \mathrm{s} = 0 \text{ for } \mathrm{i} = 1,2. \tag{32}$$

The second mixed derivative matrices N_{SR} and N_{GR} evaluated at origin (ie., s=g=0) are given by

$$N_{Sx} = \left(\frac{\partial^2 \tau_s(x_s, x)}{\partial x_{si} \partial x_{rj}}\right), \text{for } \mathrm{s} = \mathrm{g} = 0 \ \ \mathrm{i}, \mathrm{j} = 1,2, \tag{33}$$

and

$$N_{Gx} = \left(\frac{\partial^2 \tau_g(x, x_g)}{\partial x_{gi} \partial x_{rj}}\right), \text{for } \mathrm{s} = \mathrm{g} = 0 \ \ \mathrm{i}, \mathrm{j} = 1,2. \tag{34}$$

Equation (28) shows that weight function is a complex number and its phase depends on the number of caustics along the ray segments. These must be found by ray tracing and that is a reason that Kirchhoff migration needs dynamic ray tracing to correctly recover the phase of a migrated pulse (Hanitzsch, 1997).

KIRCHHOFF INVERSION BY INVERSE SCATTERING THEORY

In equation (1) the unknown true velocity $v(x)$ can be defined in terms of the background reference velocity c(x) and a velocity perturbation α(x) as:

$$\frac{1}{v^2(x)} = \frac{1}{c^2(x)}\big(1 + \alpha(x)\big). \tag{35}$$

According to Helmholtz equations (1)-(2), $\hat{\psi}_I(x, x_s, \omega)$ satisfies

$$\left[\nabla^2 + \frac{\omega^2}{c^2(x)}\right]\hat{\psi}_I(x, x_s, \omega) = -F(\omega)\delta(x - x_s), \tag{36}$$

and wave equation for $\hat{\psi}_s(x, x_s, \omega)$ from equation (1) , (35) and (36) is

$$\left[\nabla^2 + \frac{\omega^2}{c^2(x)}\right]\hat{\psi}_s(x, x_s, \omega) = -\frac{F(\omega)}{c^2(x)}\alpha(x)\hat{\psi}(x, x_s, \omega). \tag{37}$$

Here, Green function satisfies a wavefield condition traveling in from infinity

$$g(x_g, x, \omega) \sim A(x_g, x)e^{+i\omega\tau_g(x, x_g)}, \tag{38}$$

and the same for Green function of incident wavefield

$$g(x, x_s, \omega) \sim A(x, x_s)e^{+i\omega\tau_g(x, x_s)}. \tag{39}$$

Applying and rearranging Green theorem between two scalar fields of Green function equation (38) and scattered wavefield $\hat{\psi}_s(x, x_s, \omega)$, seting radiation condition, the observation data $\hat{\psi}_s(x_g, x_s, \omega)$is related to the interior values of that unknown field and unknown perturbation $\alpha(x)$ as

$$\begin{aligned}\psi_s(x_g, x_s, \omega) = -\omega^2 \int_0^\infty \frac{\alpha(x)}{c^2(x)}\big(\psi_I(x, x_s, \omega) \\ + \psi_s(x, x_s, \omega)\big)g(x_g, x, \omega)dx.\end{aligned} \tag{40}$$

Equation (40) is non-linear since it has a term that contains the product of the unknown field and perturbation (ie. $\alpha(x).\psi_s(x, x_s, \omega)$). The Born approximation linearize equation (40) by a reasonable assumption (i.e., $\alpha(x).\psi_s(x_g, x_s, \omega) \cong 0$) for small values of $\alpha(x)$ and $\psi_s(x_g, x_s, \omega)$. Now by using equations (38)-(39) it yields the following forward modeling Lippmann–Schwinger integral (or Born modeling) formula:

$$\psi_s(x_g, x_s, \omega) = -\omega^2 F(\omega)\int_0^\infty \frac{\alpha(x)}{c^2(x)}A(x, x_s(\xi))A(x_g(\xi), x(\xi))e^{-i\omega(\phi_D(x,\xi))}. \tag{41}$$

The result of Born approximation is much easier to solve since the right hand side of equation (41) does not depend on the unknown state $\psi_s(x_g, x_s, \omega)$.The perturbation value $\alpha(x)$ in the integral equation(41) can be inverted using delta function postulation approach that is well described by Beylkin (1985) and Bleistein et al., (2001). The high-frequency inversion for the velocity perturbation is obtained by assuming that source spectra is one (i.e.,$F(\omega) = 1$):

$$\alpha(x) = \frac{1}{4\pi^2}\iint d\xi^2 \frac{|h(x, \xi)|}{A(x, x_s)A(x, x_g)|\nabla_x \phi(x, \xi)|} \times \int d\omega e^{-i\omega\phi_D(x,\xi)}\psi_s(x_g, x_s, \omega). \tag{42}$$

In the above equation, the term $|h(x_r, \xi)|$ represents Beyklin determinant that is a key factor for true amplitude inversion (See Appendix A). The Beyklin determinant $|h(x_r, \xi)|$ describes the influence of source-receiver geometry. It must be finite and nonzero when high frequency inversion of integral is to be computed (Bleistein et al., 2001). Since inverting for $\alpha(x)$ causes missing of low frequency content because of its piecewise smoothness behaviour, the inversion produces bandwidth and aperture limited step functions at the positions of the reflector. The problem can be solved by inverting for reflectivity function $\beta(x)$ using the following relationship

$$\frac{\partial\alpha(x)}{\partial x_r} = -4\,\beta(x)\delta(x_r - x), \tag{43}$$

and the new inversion formula for reflectivity function is (Bleistein, 1987, 2001)

$$\beta(x) = \frac{1}{4\pi^2}\iint d\xi^2 K_B \int d\omega_{i\omega} e^{-i\omega\phi_D(x_r,\xi)}\psi_s\big(x_g(\xi), x_s(\xi), \omega\big), \tag{44}$$

where K_B is a weight function that determines the true amplitude Kirchhoff migration and is defined as

$$K_B = \frac{|h(x,\xi)|}{4\pi^2 A(x,x_s)A\big(x_g,x\big)|\nabla_x\phi(x,\xi)|}. \tag{45}$$

The reflector surface will be delineated by bandwidth and aperture limited impulses using reflectivity estimation. Using a relationship (i.e., $cos\theta = c(x)/2|\nabla_x\phi(x,\xi)|$)it is possible to derive another equivalent for reflectivity function $\beta_1(x)$ weight as by dividing K_B by $|\nabla_x\phi(x,\xi)|$

$$K_{B1} = \frac{|h(x,\xi)|}{8\pi^3 A(x,x_s)A\big(x_g,x\big)|\nabla_x\phi(x,\xi)|^2}, \tag{46}$$

which is related to $\beta(x)$ by

$$\frac{\beta(x)}{\beta_1(x)} = \frac{2cos\theta}{c(x)}, \tag{47}$$

that infers that $\beta_1(x)$ gives reflectivity information while $\beta(x)$ can give reflectivity and incident angle. Schleicher (1993) showed that his weight formula is related to the Bleistein formula in a simple relation:

$$K_{DS}(\xi,x) = K_B(\xi,x)e^{-i\frac{\pi}{2}(\kappa_S+\kappa_G)}. \tag{48}$$

The difference comes from a phase shift factor due to caustics. It is related to property of Beylkin determinant (Beylkin , 1958a) that does not allow for any caustic along ray although Creveny and Castro (1993) showed how to calculate the Beylkin determinant using dynamic ray tracing.

KIRCHHOFF INVERSION BY REVERSE-TIME METHOD AND IMAGING CONDITION

In his paper, Docherty derived the migration formula by using Green's theorem and performing a downward continuation of ψ_s. To do so, he used advanced or anticausal Green's function that has ray theoretic WKBJ approximation as

$$G(x,r,\omega) \sim A_G(x,r)e^{-i\omega\tau_G(x,r)}. \tag{49}$$

Green function for ψ_s is approximated as in equation (39). Applying Green theorem and radiation condition to ψ_s and G in the volume bounded above by the observation surface $\sum x_g$ and bellow by reflector surface Σx (ie. $\alpha(x) = 0$) now gives

$$\psi_s(r,x_s,\omega) \sim \int_{S=\sum x+\sum x_g} i\omega A_s(x,x_s)A_G(x,r))[n.\nabla\tau_s(x,x_s) + n.\nabla\tau_G(x,r)]e^{i\omega(\tau_s(x,x_s)-\tau_G(x,r))}dx^2, \tag{50}$$

where n is a unit normal to surface $\sum$ and the phase is

$$\phi(x,x_s,r) = \tau_s(x,x_s) - \tau_g(x,r). \tag{51}$$

The main contribution to the integral comes from such a zone surrounding ξ_0 that the phase $\phi(\xi)$ is stationary

$$\frac{\partial\phi}{\partial\xi_i} = (\nabla\tau_s - \nabla\tau_G).\frac{\partial x}{\partial\xi_i} = 0 \quad i = 1,2. \tag{52}$$

In stationary points the slowness vectors $\nabla\tau_s$ and $\nabla\tau_G$ and the normal component of surface *n* should satisfy $n.\nabla\tau_s = n.\nabla\tau_G$ on stationary surface S_0 and $\mathrm{n}.\nabla\tau_s + n.\nabla\tau_G = 0$ on reflector surface $\sum x$. Evaluation of $\psi_s$on reflector surface is zero and major contribution of the integral comes from observation surface $\sum x_g$. This implies that for a upgoing scattered wavefield $\psi_s(r,x_s,\omega)$, where *r* is above the reflector it is always possible to find a point on observation surface $\sum x_g$ that stationary condition satisfied (Docherty, 1991) . Using $n.\nabla\tau_s = n.\nabla\tau_G$ and the relationship $\frac{\partial\psi_s}{\partial n} \sim i\omega n.\nabla\tau_s$ at stationary point equation (50) changes to

$$\psi_s(r,x_s,\omega) \sim 2i\omega \int_{\sum x_g} A_G(x,r)[n.\nabla\tau_G(x,r)]e^{-i\omega(\tau_G(x,r))}\psi_s(r,x_s,\omega)ds. \tag{53}$$

The integral over surface $\sum x_g$ produces a wave which propagates downwards, continues even bellow the reflector, as the time is reversed.

After downward continuation of the ψ_s along with the forward model of the source point at a reflector, layer property can be estimated by imaging condition that defined by Claerbout (1971). This is obtained by dividing the scattered wavefield $\psi_s(r,x_s,\omega)$ just above the reflector by the incident wavefield $\psi_I(r,x_s,\omega)$ just before the reflector. In the time domain the imaging condition is the crosscorelation between $\psi_I(\xi,t)$ and $\psi_s(\xi,t)$.

The significance of this method is the foundation of imaging condition inversion to get the reflectivity. Figure 5 illustrates kinematics behind downward continuation (in time domain) of the scattered field back to reflection point where the imaging condition can create reflectivity.

By implementing the imaging principle at every image location between the source and receiver wavefields the migration output m(r) is obtained from

$$m(r) \sim \frac{1}{2\pi}\int F(\omega)\frac{\psi_s(r,x_s,\omega)}{\psi_I(r,x_s,\omega)}d\omega, \tag{54}$$

by WKBJ approximation and using equation(39) for ψ_s the 3-D Kirchhoff migration algorithm is derived as

$$\mathrm{m(r)} \sim \frac{1}{\pi A_I(r,x_s)} \int_{\sum x_g} dx^2 A_G(x,r)[n.\nabla\tau_G(x,r)] \times \int d\omega\, i\omega\, F(\omega) e^{-i\omega[\tau_I(x,x_s)+\tau_G(x,r)]} \psi_s(x,x_s,\omega)\,. \tag{55}$$

Docherty (1993) proved that Blestein's inversion formula for common shot configuration is identical to his formula using the following relationship:

$$\frac{|h(y,\xi)|}{|\nabla_y \phi(y,\xi)|^2} = A^2{}_G(x,r) 8\pi^2 \sqrt{g}\, n.\nabla\tau_G(x,r), \tag{56}$$

where quantity $\sqrt{\mathrm{g}}$ is differential surface area and is defined as $\sqrt{g}\, d\xi_1 d\xi_2 = dS$.

This approach is limited only to common source configuration inversion because of limitation on imaging condition. The other disadvantageous is that the reverse-time method has grid dispersion problems and may require a smaller trace interval, and thus require more computational time (Bancroft, 2000).

WEIGHT FUNCTIONS FOR COMMON SOURCE CONFIGURATIONS

In this section three weight functions derived by Schleicher (Schleicher et al., 1993) , Bleistein (Bleistein et al. 1985, 1987, 1987a, 1987b) and Docherty (Docherty, 1993) on a common source configuration are compared. The ray reflected from the horizontal homogenous model with thickness of ***h*** from a half space with constant migration velocity model (see e.g., Figure 6).

In this case we ignore the existence of caustic. For common source configuration we should set $\Gamma_S^T = 0$ since source is fixed (i.e., $\frac{\partial s_i}{\partial \xi_1} = 0$) and $\Gamma_G^T = I$, (i.e $\frac{\partial g_i}{\partial \xi_1} = \mathrm{I}$). As described by Schleicher (2007) we get

$$K_{DS}(\xi;x) = \sqrt{\frac{\cos\vartheta_S \cos\vartheta_G}{\upsilon_S \upsilon_G} \frac{|det\,(N_{Gx}|}{\sqrt{|det\,(N_{Sx}|}\sqrt{|det\,(N_{Gx}|}}}, \tag{57}$$

which is equivalent to:

$$K_{DS}(\xi;M) = \sqrt{\frac{\cos\vartheta_S \cos\vartheta_G}{\upsilon_S \upsilon_G} \frac{\sqrt{|det\,(N_{Gx}|}}{\sqrt{|det\,(N_{Sx}|}}}. \tag{58}$$

By rearranging equation (57) for two ray segments from source to reflector and from reflector to the receiver ray segment geometrical we have

$$\sqrt{|det\,(N_{Sx}|} = \sqrt{\frac{\cos\vartheta_S \cos\vartheta_G}{\upsilon_S \upsilon_G} \frac{1}{|\mathcal{L}_S|}}, \tag{59}$$

and

$$\sqrt{|det\,(N_{Gx}|} = \sqrt{\frac{\cos\vartheta_S \cos\vartheta_G}{\upsilon_S \upsilon_G} \frac{1}{|\mathcal{L}_G|}}, \tag{60}$$

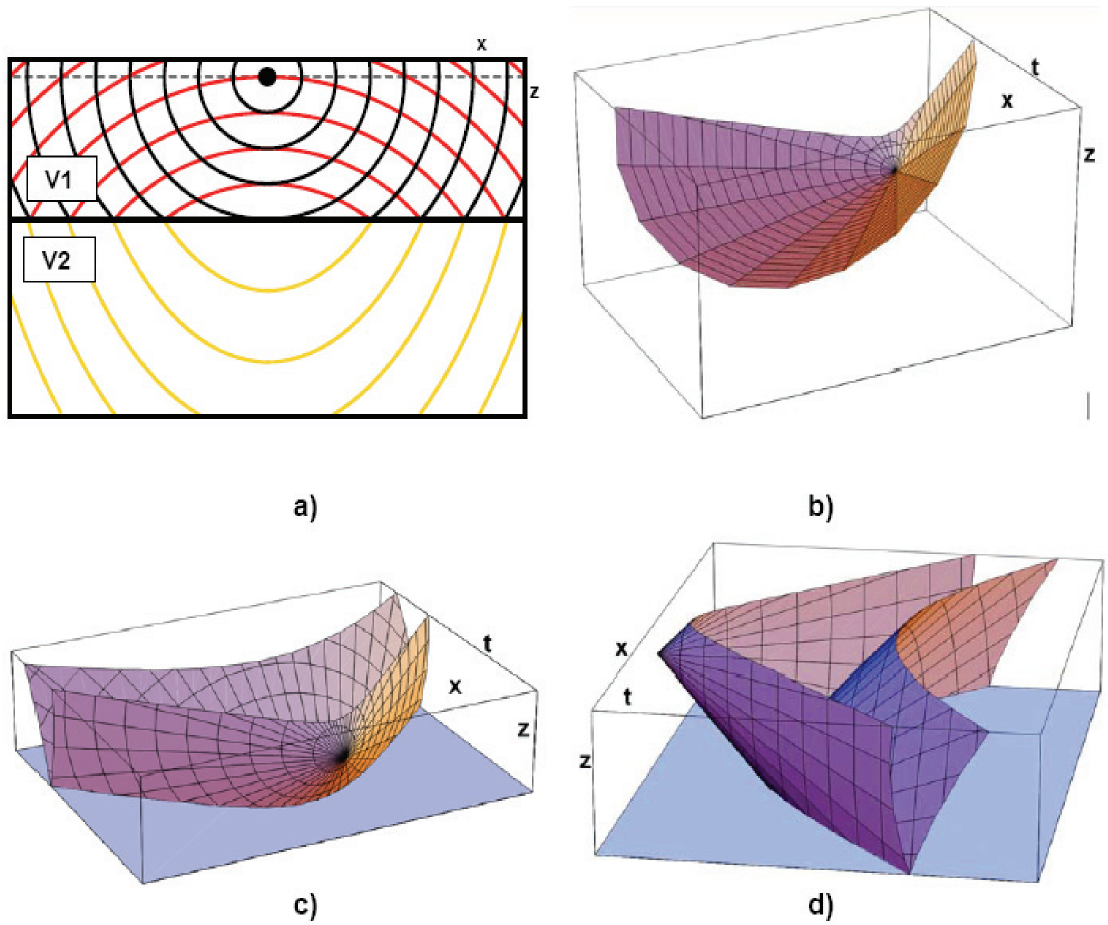

FIG.5. Wavefront model for a horizontal reflection and downward continuation of scattered field with a) showing a multiple exposure of the incident wavefield $\psi_I(\xi,t)$ and the scattered wavefield $\psi_s(\xi,t)$, b) the incident wavefield $\psi_I(\xi,t)$, c) the combined $\psi_I(\xi,t)$ and $\psi_s(\xi,t)$ energy in perspective view, and d) an alternate perspective view of (c) The black, blue and yellow curves in (a) represents incident, reflected and transmitted waves(Bancroft, 2000).

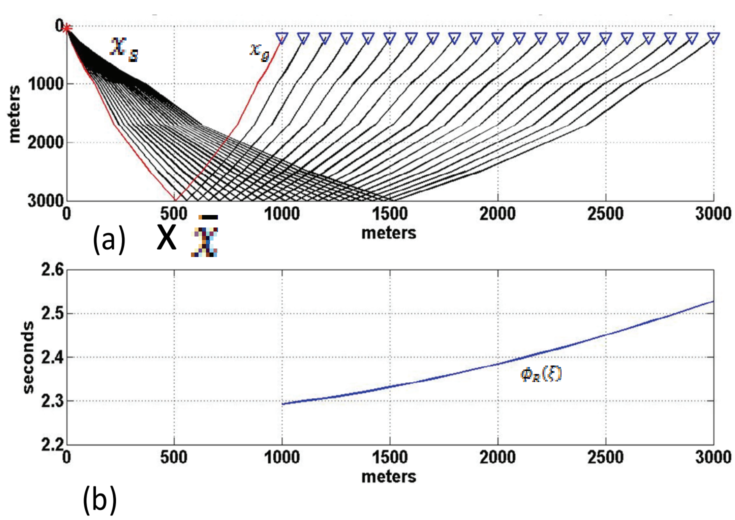

FIG. 6. Simulation for common source configuration for a flat reflector.(a) The ray paths (b) Reflection traveltime ϕ_R.

Substituting (59 & 60) into (58) gives

$$K_{DS}(\xi;\mathrm{x}) = \frac{\cos\vartheta_G}{\upsilon_G}\frac{|\mathcal{L}_s|}{|\mathcal{L}_G|}. \tag{61}$$

Keho and Beydoun (1988) derived similar weight function for common-source for our model as

$$K_{DS}(\xi;\mathrm{x}) = \frac{\cos\vartheta_G}{\upsilon_G}\frac{A(x,x_g)}{A(x,x_s)}. \tag{62}$$

Sun and Gajewski (1997) approximated ratio of $|\mathcal{L}_s|$ and $|\mathcal{L}_G|$ based on concept of ray tube (which is a tube whose walls are defined by an infinite number of infinitesimally closely spaced ray emerging from source point)as

$$\frac{|\mathcal{L}_s|}{|\mathcal{L}_G|} = \frac{cos\,\vartheta_G}{cos\,\vartheta_s}. \tag{63}$$

Now the final weight function is

$$K_{DS}(\xi;M) = \frac{cos^2\,\vartheta_G}{\upsilon_G\,cos\,\vartheta_s}. \tag{64}$$

In Beylkin determinant (see appendix A) for CS configuration since source slowness p_s is independent of surface ccordinates the beylkin determinant changes to

$$|h(x,\xi)| = \begin{vmatrix} p_s + p_G \\ \frac{\partial}{\partial \xi_1}(p_G) \\ \frac{\partial}{\partial \xi_2}(p_G) \end{vmatrix}, \tag{65}$$

which can be further simplified to

$$|h(x,\xi)| = 2\,cos^2\,\theta \begin{vmatrix} p_G \\ \frac{\partial}{\partial \xi_1}(p_G) \\ \frac{\partial}{\partial \xi_2}(p_G) \end{vmatrix}. \tag{66}$$

For convenience the ray path from source to scatterpoint is $(r_s = x_s x)$ and ray path from scatterpoint to receiver is denoted by $(r_g = x_g x)$. In a constant velocity model the travel time is $\phi_D(x,\xi) = \frac{r_s + r_g}{c}$ and $\frac{\partial r_s}{\partial \xi_i} = 0$, Bylkein determinant simplifies to:

$$|h(x,\xi)| = \frac{2\cos^2\theta}{c^3 r_g^2} \begin{vmatrix} r_G \\ \frac{\partial}{\partial \xi_1}(r_G) \\ \frac{\partial}{\partial \xi_2}(r_G) \end{vmatrix}. \tag{67}$$

Since the acquisition surface is flat and no topographic variation exist here the vector variations of x_g is $x_g = (\xi_1, \xi_2, 0)$, it turns out to $\frac{\partial}{\partial \xi_1}(x_g) = (1,0,0)$, $\frac{\partial}{\partial \xi_2}(x_g) = (0,1,0)$.

Considering the emergence angle ϑ and azimuth angle α as shown in Figure 2, the vector r_g is obtained by

$$r_g = (sin\,\tilde{\theta}\,cos\,\alpha\,, sin\,\tilde{\theta}\,sin\,\alpha,\; cos\,\tilde{\theta}). \tag{68}$$

Using $cos\,\vartheta = \frac{h}{r_g}$ it is possible to calculate the Beylkin determinant as

$$|h(y,\xi)| = \frac{2\cos^2\theta h}{\upsilon^3 r_g^3}. \tag{69}$$

that leads to the final weight function

$$K_B = \frac{2\cos\theta h r_s}{\pi\upsilon^2 r_g^2} \text{ or } K_{B1} = \frac{h r_s}{\pi\upsilon r_g^2}. \tag{70}$$

Comparing with K_{DS} in our model, since $r_s = r_g$and $\vartheta_G = \vartheta_s$ we have $K_B \propto K_{DS}$. Docherty formula produces the same result since $n.\nabla\tau_G(x,r) = \cos\vartheta\,/\upsilon$ and $A_G(x,r) = A_I(r,x_s)$. The scaling factor does not affect the trend of reflectivity estimation. This means all three weight functions are the same.

CONCLUSIONS

The methods of paraxial ray theory (Schleicher, 1993), inverse scattering (Bleistein et al., 1987) and applying imaging condition on downward continuation of seismic data (Docherty, 1991) result in the similar algorithm. They use similar weight function for diffraction stack process if the caustics are not present. In the case of caustics along the ray path Schleicher (1993) weight function works properly, in contrast because of properties of Beylkin determinant the weight function by Bleistein et al.,(1987) and Docherty (1991) do not count any caustic along the rays.

ACHNOWLEDGEMENTS

The authors would like to thank all CREWES sponsors for their supports. We want to thank Faranak Mahmoudian and Hugh Geiger for their helpful discussions and suggestions on this subject. The comments of Dr. Edward S. Krebes on ray theory are very much appreciated.

REFERENCES

Bancroft,J.C.,2000, course note “A practical understanding of prestack Migration”: University of Calgary

Beylkin, G., and Burridge, R., 1990, Linearized inverse scattering problems in acoustics and elasticity: Wave Motion, **12**, 15-52.

Bleistein, N., 1987, On the imaging of reflectors in the earth: Geophysics,**52**, 931–942.

———1987, On the imaging of reflectors in the earth: Geophysics, **52**,931–942.

Bleistein, N., Chohen, J. K., Stockwell, Jr., 2001, Mathematics of multidimensional seismic imaging, migration and inversion: Springer Press Inc.

Bleistein, N., Cohen, J. K., and Hagin, F. G., 1987, Two and one-half dimensional Born inversion with an arbitrary reference: Geophysics, **52**, 26-36.

Bortfeld, R., 1989, Geometrical ray theory: Rays and traveltimes in seismic systems (second-order approximation of the traveltimes): Geophysics, **54**, 342-349.

Cerveny, V., 2001, seismic ray theory: Cambridge University Press Inc.

Cerveny, V., Castro M.,2001, application of dynamic ray tracing in the 3-D inversion of seismic reflection data: Geophys. J. Int., **113**,776-779.
Claerbout, J. F., 1985, Imaging the earth's interior: Blackwell Scientific Publications, Inc.
Docherty, P., 1991, A brief comparision of some Kirchhoff integral formulas for migration: Geophysics, **56**, 1164-1169.
Goldin, S. V., 1986, Seismic traveltime inversion, Soc. Expl. Geophys. Monograph.
Hanitzsch, C., Hubral, P., Schleicher, J., and Tygel, M., 1992, True-amplitude migration of 2-D synthetic seismograms, 47th Ann. Internat. Mtg., Europ. Assoc. Expl. Geophys., Expanded Abstracts, 276-277.
Hanitzsch, C., Schleicher, J., and Hubral, P., 1994, True-amplitude migration of 2-D synthetic data: Geophys. Prosp., **42**, 445–462.
Hanitzsch, C., 1997, Comparison of weights in prestack amplitude-preserving Kirchhoff depth migration: Geophysics, **62**, 1812–1816.
Hubral, P., Schleicher, J., and Tygel, M., 1992, Three-dimensional paraxial ray properties—I: Basic relations: J. Seis. Expl., **1**, 265–279.
Jaramillo H. H., Bleistein N., 1999, The link of Kirchhoff migration and demigration to Kirchhoff and Born modeling: Geophysics, **64**, 1793–1805.
Margrave, G. 2010, Inversion course note: university of Calgary
Schleicher, J.,Tygel, M., and Hubral,P., 1993, 3-D true-amplitude finite offset migration: Geophysics, **58**, 1112–1126.
Krebes, E. S., 2009, Theoretical seismology, lecture notes: university of Calgary
Schleicher, J.,Tygel, M., and Hubral,P., 2007, Seismic true amplitude imaging: Society of Exploration Geophysicists
Schneider, W. A., 1978, Integral formulation for migration in two and three dimensions: Geophysics, **43**, 49-76.
Shearer, P. M., 1999, Introduction to seismology: Cambridge University Press.
Sun, J., 1994, Geometrical ray theory: Edge-diffracted rays and their traveltimes (second-order approximation of the traveltimes): Geophysics, **59**, 148–155.
Sun, J., and Gajewski, D., 1997, True-amplitude common-shot migration revisited: Geophysics, **62**, 1250–1259.
———1998, On the computation of the true amplitude weighting functions: Geophysics, **63**, 1648–1651.

APENDIX A: SOME PROPERTIES OF BEYLKIN DETERMINANT

Beylkin determinant reveals a close relationship to true amplitude migration. It is defined as (Bleistein et al, 2001)

$$|h(x,\xi)| = \begin{vmatrix} p_s + p_g \\ \frac{\partial}{\partial \xi_1} \nabla_x (p_s + p_g) \\ \frac{\partial}{\partial \xi_2} \nabla_x (p_s + p_g) \end{vmatrix}. \quad \text{(A-1)}$$

By defining the following quantities the above equation can be further simplified

$$h(y,\xi) \equiv (p_s + p_g).\left[(v_s + v_g) \times (w_s + w_g)\right], \quad \text{(A-2)}$$

where $v_s \equiv \frac{\partial p_s}{\partial \xi_1}, v_g \equiv \frac{\partial p_g}{\partial \xi_1}\ , w_s \equiv \frac{\partial p_s}{\partial \xi_2}\ and\ w_g \equiv \frac{\partial p_g}{\partial \xi_2}$. Therefore, the Beylkin determinant is expressed by triple scalar product of three vectors. By definition of derivative and cross product of the above vectors the following triple scalar product relations exists:

$$p_g.(v_s \times w_s) = \frac{\mu_s \cos 2\theta}{c(y)} |v_s \times w_s|, \tag{A-3}$$

and

$$p_s.\left(v_g \times w_g\right) = \frac{\mu_g \cos 2\theta}{c(y)} \left|v_g \times w_g\right|. \tag{A-4}$$